Land-Atmosphere Interactions Exacerbated the Drought and Heatwave over Northern Europe during Summer 2018

Paul A. Dirmeyer

Center for Ocean-Land-Atmosphere Studies, George Mason University, Fairfax, Virginia, USA

Gianpaolo Balsamo

European Centre for Medium-range Weather Forecasts, Reading, United Kingdom

Eleanor M. Blyth, Ross Morrison, and Hollie M. Cooper

UK Centre for Ecology and Hydrology, Wallingford, United Kingdom

Abstract

The 2018 drought and heatwave over Europe was exceptional over northern Europe, with unprecedented forest fires in Sweden, searing heat in Germany and water restrictions in England. Monthly, daily and hourly data from ERA5, verified with *in situ* soil moisture and surface flux measurements over Britain, are examined to investigate the subseasonal-to-seasonal progression of the event and the diurnal evolution of tropospheric profiles to quantify the anomalous land surface contribution to heat and drought. Data suggest the region entered a rare condition of becoming a “hot spot” for land-atmosphere coupling, which exacerbated the heatwave across much of northern Europe. Land-atmosphere feedbacks were prompted by unusually low soil moisture over wide areas, which generated moisture limitations on surface latent heat fluxes, suppressing cloud formation, increasing surface net radiation and driving temperatures higher during several multi-week episodes of extreme heat. We find consistent evidence in field data and reanalysis of a breakpoint threshold of soil moisture at most locations, below which surface fluxes and daily maximum temperatures become hypersensitive to declining soil moisture. Similar recent heatwaves over various parts of Europe in 2003, 2010 and 2019, combined with dire climate change projections, suggest such events could be on the increase. Land-atmosphere feedbacks may play an increasingly important role in exacerbating extremes, but could also contribute to their predictability on subseasonal time scales.

Plain Language Summary

This study uses a combination of environmental observations over Britain, atmospheric and land surface analyses over Europe to examine the exceptional drought and heatwave over northern Europe during the summer of 2018. Results suggest the region entered a state of positive feedback between the land and atmosphere, exacerbating the heatwave over the area. This is a situation that is common over southern Europe and many other places in the world, but rare for northern Europe. Dry soils and vegetation led to reduced evaporation, increased heating of the surface, warming and drying of the air, contributing to less cloud cover. Particularly, a breakpoint value of soil moisture has been found for most locations, below which evaporation, heating and daily maximum temperatures become significantly more sensitive to declining soil moisture. This is both a worrying indicator for the region in a warming climate and a potential source of additional predictability for the intensification of future heatwave events.

1. Introduction

The summer of 2018 saw a combination of drought and heat concentrated on northern Europe. The conditions had far-reaching economic and ecological impacts, with spring and summer dryness affecting crops and natural vegetation, increased tree and forest mortality, including unprecedented wildfires particularly in Sweden (Clément Albergel et al., 2019; Rösner et al., 2019). The atmospheric circulation began to establish conditions for anomalous heat and drought in the spring, with blocking high pressure and unfavorable moisture sources for precipitation beginning in April (Rösner et al., 2019). European heatwaves are associated with such mid-latitude quasi-stationary wave patterns (Wolf et al., 2016), but advection can also play a significant role (Sousa et al., 2019). Synoptic features of the heatwave were well forecast up to two weeks in advance, and some aspects were evident out to four weeks (Magnusson et al., 2018), suggesting its origins were in the large-scale hemispheric circulation (Kornhuber et al., 2019).

The combined hot and dry conditions experienced in northern Europe are more typical of southern Europe, but such situations are projected to become more common in a changing climate (Samaniego et al., 2018; Teuling, 2018; Zscheischler et al., 2018). For example, the summer of 2018 was among the warmest, sunniest and driest on record in the UK (Kendon et al., 2019). A regional modeling study has suggested some of the heatwave signal over Britain may be attributable to the effect of regional sea surface temperature anomalies (Petch et al., 2020). The same study suggests local soil moisture anomalies had nearly as large an impact on temperatures. Northern Europe is not a region which typically experiences land-atmosphere coupling that promotes positive feedbacks in situations such as droughts or heatwaves (Seneviratne et al., 2010). Could it be that northern Europe entered into an unprecedented positive feedback regime during the summer of 2018?

There is generally a positive relationship between soil dryness and heat (Fischer et al., 2007; Hirsch et al., 2014; Philip et al., 2018; Santanello et al., 2011). Obviously high temperatures are conducive to drying the soil by increasing the evaporative demand by the atmosphere. But there is a positive feedback – dry soils heat more quickly than wet ones and may thus transmit absorbed radiant energy to the atmosphere as sensible heat more readily than wet soils, as the gradient between surface and near-surface air temperatures can become larger. Furthermore, dry soils correspond to reduced evaporation, and if dry enough to sufficient depth, reduced transpiration by plants. This reduces evaporative cooling potentially further exacerbating the heat (Dirmeyer et al., 2015). In general, land surface states and soil moisture can be a source of such feedbacks when water availability in the soil is a limiting or controlling factor for evapotranspiration, while the land is not a factor in energy-limited situations such as when conditions are wet, cool and cloudy (Santanello et al., 2018).

It is through the processes that permit soil moisture variations to affect surface heat fluxes and near-surface meteorological states that land surface feedbacks to the atmosphere occur (Dirmeyer, Gentine, et al., 2018). The feedbacks also alter the daytime boundary layer, which can ultimately affect cloud formation, precipitation, and the state of the free atmosphere above the boundary layer (Santanello et al., 2011). When and where there is atmospheric sensitivity and responsiveness to changes in the land state, the land becomes a source of predictability for the atmosphere, a "hot spot" of land-atmosphere coupling (Koster et al., 2006). In the case of droughts and heatwaves, the land surface can be a source of persistence and intensification of the extreme states (Miralles et al., 2018). These effects are most important when radiative energy is most abundant. In mid-latitudes this is during late spring and summer, and diurnally it is during the daylight hours. The diurnal evolution of the atmospheric boundary layer over land is driven by sensible heating of the atmosphere from contact with the surface (Santanello et al., 2009). Many past studies have concentrated on the daylight hours and processes active at that time (Betts, 2004; Ek & Holtslag, 2004; Gentine et al., 2013; Santanello et al., 2007; Zhang et al., 2020). Adequate temporal resolution of the diurnal cycle is key for such studies.

Over Europe, recent years have seen several episodes of unprecedented heat (Russo et al., 2015), and future climate projections strongly suggest a positive trend for such events (Lau & Nath, 2014; Seneviratne et al., 2006). Over northern Europe there is particular concern, as there is little history of such events. Although warning systems are being implemented, infrastructure is not designed or well prepared to cope with heatwaves (Casanueva et al., 2019; Lass et al., 2011). Drought has also been a much more common event in southern Europe than northern Europe (Vicente-Serrano et al., 2014). While positive trends in drought are indicated in both regions, with drying common to majority of land areas (Albergel et al., 2013) the unfamiliarity with such extremes in the North introduces additional challenges.

Modeling studies indicate that most of northern Europe is usually in an energy-limited regime, even during the warmer summer months, and thus not responsive to soil moisture anomalies (Dirmeyer et al., 2009; Schwingshackl et al., 2018). This is because there is a range of soil moisture over which a fairly linear and decidedly monotonic relationship exists with latent heat fluxes. Above a certain value of soil moisture, the dependence of latent heat on soil moisture diminishes or disappears. Likewise, there is a lower bound of soil moisture below which latent heat flux shuts down. These thresholds are often associated with the field capacity and wilting point respectively, although latent heat flux may fail to increase with increasing soil moisture below field capacity if insufficient net radiation is available to drive maximum evapotranspiration – this is often the case in northern Europe.

Given the concurrent dry and warm conditions over much of northern Europe during the summer of 2018, we pose the question: Did northern Europe enter a regime of land surface feedbacks to the atmosphere – i.e., did it become a "hot spot" that may have intensified the heatwave? We combine analysis of *in situ* observational data and state-of-the-art gridded reanalyses to investigate the question. Section 2 describes the data used. Analysis techniques and metrics of land-atmosphere interaction are presented in Section 3. Results are shown in Section 4, followed by conclusions in Section 5.

2. Data

Hourly data from the European Centre for Medium-range Weather Forecasts (ECMWF) ERA5 covering the 40-year period 1979-2018 are used in this study (Hersbach et al., 2020). The data are at a nominal 31 km resolution but have been interpolated back to the full TL639 grid (~0.28°) for this analysis. Vertical resolution is also higher than any previous reanalysis, with 23 layers in the lowest 15% of the atmosphere by mass, and 55 layers in the lowest 70%.

ERA5 is the first reanalysis to assimilate satellite soil moisture data (de Rosnay et al., 2014). This assures better quality analyses of soil moisture, but also assures a lack of closure of the terrestrial water balance. Nevertheless, reanalyses have been shown to perform well in regard to the simulation of land-atmosphere coupling metrics based on daily data (Dirmeyer, Chen, et al., 2018). ERA5 provides the opportunity to examine the diurnal cycle with unprecedented detail as hourly data for all atmosphere and land surface variables are available. The diurnal cycle is a key element of coupled land-atmosphere processes (Santanello et al., 2018). The 12-hour data assimilation windows are shifted 6 hours from the 0000 and 1200UTC windows used in previous reanalyses, and artifacts are sometimes evident toward the end of those windows, as is shown in Section 4. Note that because of lack of local budget closure in the reanalysis fields, exact budgets cannot be calculated. Nevertheless, a good depiction of the temporal variability in budget terms is afforded.

For *in situ* analysis and comparisons over Britain, data from two grassland flux towers in southern England operated by the UK Centre for Ecology and Hydrology (UKCEH) are used. The eddy covariance instrumentation combines Gill Instruments Ltd. (Lymington, UK) ultrasonic anemometer-thermometers and LI7500 series infrared gas analyzers (Li-COR Biosciences, Nebraska, USA), alongside a standardized set of micrometeorological (radiation, air temperature, humidity and pressure) and soil physics (temperature, moisture and heat flux) sensors. Data processing and quality control follow methods of the global flux measurement community (Fratini & Mauder, 2014; Papale et al., 2006; Reichstein et al., 2005). Full details of the measurement sites, instrumentation and data handling can be downloaded with the eddy covariance datasets (Morrison et al., 2019, 2020). The data duration is short compared to ERA5, but provides ground truth to validate aspects of the coupled land-atmosphere behavior in ERA5 – fidelity lends confidence to the larger-scale analyses. As with ERA5, energy and water budgets from the eddy covariance sites do not close, but well-managed flux tower sites can still have great value for assessing local heatwave maintenance processes (Horst et al., 2019).

UKCEH also maintains a network of large-area soil moisture monitoring sites (COSMOS-UK), with collocated meteorological observations, that is based on the cosmic ray neutron sensor. The COSMOS-UK network has been developed since 2013 and provides sub-daily field scale soil moisture, derived from fast neutron counts at the land surface (Stanley et al., 2019). Near surface soil moisture is determined using corrections for local atmospheric pressure, humidity and background neutron intensity (Evans et al., 2016; Rosolem et al., 2013), and site-specific calibration based on destructive soil sampling (Evans et al., 2016). The COSMOS-UK network is more extensive than the flux towers, providing a distributed picture of near-surface water storage over Britain. Figure 1 provides a map of all site locations used in this analysis (Antoniou et al., 2019). Additionally, surface fluxes have been estimated for some COSMOS-UK sites; where sensible heat flux is derived from eddy covariance instrumentation, and latent heat flux estimated as a residual from the other terms of the surface energy budget measured at COSMOS-UK sites (Crowhurst et al., 2019).

Such *in situ* measurements provide ground truth at a small number of locations around Britain, which are used to validate the behavior of ERA5 data that provide complete coverage over the entire domain of interest. Tables S1 and S2 show the temporal correlations of daily time series between observations and ERA5 for soil water content and daily maximum temperature at the COSMOS-UK sites, and for a number of variables at the flux tower sites. Correlations are calculated separately for 2017 and 2018 for the warm season period spanning 15 May through 15 October – a period of 154 days. In every case, the correlations are significant at the 99% confidence level, suggesting ERA5 provides a trustworthy univariate representation of states and fluxes near the surface. Multivariate behavior, which is a crucial indicator of processes linking land and atmosphere, is the topic of study in results section.

3. Metrics

In order to investigate the possible role of land-atmosphere feedbacks on the 2018 heatwave and drought, we estimate several land-atmosphere coupling metrics as well as energy budget terms over affected areas. Anomalies in temperature, volumetric soil water content, and fluxes are calculated relative to a 40-year (1979-2018) climatological period for ERA5 data. For *in situ* data over Britain, comparisons between corresponding periods in 2018 and 2017 are made, as long records are not available from the relatively new networks.

Daily data are used to produce areal averages of key heat and moisture budget terms averaged over selected regions. Surface and atmospheric budgets are produced on an hourly timescale averaged over Britain to derive mean diurnal cycles of surface and vertical heating profiles. The

ERA5 land mask is used to define the areal domains as land grid cells only, and averages across the grid cells are area weighted. For the vertical profiles of atmospheric variables, calculations are performed on the native ERA5 vertical levels, whose thicknesses at any location are proportional to surface pressure (i.e., a sigma coordinate in the vertical). The vertical dimension over Britain is rendered in the model coordinate as values relative to a surface pressure of 1013.25 hPa, but are in fact usually somewhat smaller, especially over elevated terrain.

Lifted condensation level (LCL) is compared to the depth of the planetary boundary layer (PBL) to determine an LCL deficit (Santanello et al., 2011). We define it here with the opposite sign from its original specification, such that negative values indicate the PBL does not grow deep enough for condensation and cloud formation to occur at its top. Such a shortfall can be caused by either insufficient heating at the surface to generate the necessary buoyancy, low relative humidity of air near the surface, or a combination of both.

Segmented regression is used to determine if there is a significant change in the relationship between soil moisture and extreme temperatures or surface fluxes that can be attributed to land-atmosphere feedbacks (Wu & Dirmeyer, 2020). Figure 2 provides an example at one ERA5 grid cell: for a specific time period (in this case a particular calendar month across 40 years), daily values of surface (0-7 cm) volumetric soil moisture and daily maximum air temperature are seen to have an inverse relationship, which is typical of many mid-latitude locations. To determine whether there is a difference in the slope of temperature estimated over different ranges of soil moisture, an optimization is calculated to minimize the RMS error of a pair of linear regressions over two segments which together cover the entire range of soil moisture at that grid cell and month (V. M. Muggeo & Hajat, 2009; V. M. R. Muggeo, 2003). The criterion is that the two linear regressions must intersect at the same value of temperature (red dot) at the soil moisture breakpoint between the segments (red line). Optimization is performed over four parameters: the slopes of the left (drier) and right (wetter) segments, the breakpoint values of soil moisture and maximum temperature.

Additional criteria are applied to filter the results. First, the two slopes must be significantly different. The variances of the estimates of the two slopes are averaged after adjusting down the sample size of N days by the soil moisture memory τ in days as $N/(\tau + 1)$, to properly account for the degrees of freedom. From that, a z-score and p-score are calculated assuming a normal distribution of the potential errors in parameter estimates; p-scores of 0.01 or less are retained. Because we have in mind specific physical processes by which low soil moisture may affect air temperature, we further constrain that the slope of the linear regression to the left of the estimated breakpoint be negative for temperature or sensible heat flux, positive for latent heat flux or evaporative fraction, and that the slope have a larger magnitude on the drier side of the breakpoint than the wetter side. We also check that there are at least 10 data points on either side of the breakpoint. Locations where the optimization fails to converge are omitted.

4. Results

A question emerges for the summer of 2018: did locations in northern Europe move into a regime where land surface feedbacks exacerbated drying and warming? First, the degree of the extremities for summer 2018 are determined. Figure 3 shows the fraction of the 122 days of May through August 2018 that lie within the indicated tails of maximum 2m air temperature anomalies and surface (top 7 cm) volumetric soil water content, based on ERA5. By chance, one would expect a value of 0.05 at any location in the maximum temperature plot, and 0.25 for soil water content. There is strong spatial correspondence between the two panels, but the core or dry soils is clearly south of the core of high temperatures. In parts of Germany, nearly every day of May-August 2018 are in the driest quartile. For temperature, the most extreme conditions were over southern Scandinavia, where up to one third of the period was in the warmest 5% of anomalies of the previous 40 years. Each panel shows large areal coverage of significant anomalies, yet much of Eastern Europe is significantly dry but not significantly warm.

The evolution of monthly mean anomalies in surface volumetric soil moisture and maximum 2 m air temperature over land are shown in Figure 4 for the period of May-August 2018. Anomalously warm and dry conditions predominate over northern Europe in each month, but the patterns are not stationary. For soil moisture, only areas around northern Germany and the Baltic states are more than 0.03 drier than average in every month. Areas of positive temperature anomalies alternate between extreme heat over Scandinavia and lands adjacent to the North and Baltic seas (May, July) and less intense but still widespread warm anomalies anchored around Germany (June, August).

A more complete picture is given in supplemental figures Figures S1-S3, which portray anomalies in boundary layer states, surface energy and moisture fluxes as represented in ERA5. Precipitation and soil moisture evolve similarly, while anomalies in surface turbulent heat fluxes are much more prominent in sensible than latent heat flux (Figure S1). Increases in sensible heat flux correspond strongly with positive anomalies in downward shortwave radiation (Figure S2). Meanwhile, latent heat flux deficits are more closely linked to extremely dry soil, particularly during July and August. The planetary boundary tends to be slightly deeper in most regions (Figure S3) but is outpaced by the increases in the lifted condensation level, hampering cloud formation in areas where downward shortwave radiation increases.

There was considerable synoptic variability in heatwave and drought conditions during 2018 and the use of monthly means does not capture the nuances nor the peak periods. Nevertheless, the preceding figures give a good first-order impression of the magnitude and duration of warm dry conditions over northern Europe during the period.

Focusing on three areas that bore the brunt of the hot conditions: Southern Scandinavia (hereafter SSc), the Northern European Plain (NEP) and the island of Britain (all outlined in Figure 3), Figure 5 presents area averages of daily time series during May-August. The top row shows volumetric surface soil moisture for 2018 relative to its 40-year (1979-2018) climatological evolution, simply calculated as daily means with a centered 7-day running average applied. Each region was predominantly drier than normal, with the greatest anomalies during the first half of July. SSc also had a dry period during late May and early June that was as intense as during July, while NEP also saw very dry conditions in late July and August. Britain's driest period spanned from late June to late July. The second row shows the climatological and 2018 accumulated precipitation from 1 May onwards, showing extreme shortfalls in all regions, although both SSc and Britain showed rainfall rates returning to normal in August (matching slopes of the curves).

Area averaged daily maximum temperatures are shown in the middle row of Figure 5. Positive anomalies dominate in all regions. Heatwave peaks correspond largely to the periods of lowest soil moisture except over NEP where the late May heat was during a period clearly wetter than the early July dry period during which temperatures were mainly 1-5°C above average rather than 8-10°C. The fourth row shows the LCL deficit (Santanello et al., 2011): negative values indicate the boundary layer does not grow deep enough for condensation and cloud formation to occur. The climatological lines show deficits hovering around 0 m over SSc and NEP, and consistent positive values over Britain suggesting clouds are likely to form above a growing boundary layer during every day of the period. During 2018, deficits predominate over SSc and NEP, as well as during the most intense heatwave periods over Britain, where summer values were usually well below climatology. From Figure S3 it can be seen that the main cause was elevated LCL heights due to warm dry air, as PBL growth was not suppressed markedly during the period and was often above average.

The periods lacking convective clouds over land correspond to anomalous increases in downward shortwave radiation at the surface (Figure 5, bottom row). Those are also periods of enhanced sensible heat flux in ERA5, but latent heat flux is not as responsive to the fluctuations in radiation. In fact, an interesting reversal occurs around July 1. Before that period, latent heat flux is clearly positively correlated with shortwave radiation, suggesting evaporation is limited by available energy. This is the typical situation across northern Europe. After 1 July, latent heat flux becomes anticorrelated with both shortwave radiation and sensible heat flux, indicative of a moisture-limited situation. This is a necessary condition for land-atmosphere feedback (Dirmeyer et al., 2015), suggesting a rare and possibly unprecedented situation of the development of a coupling "hot spot" from land to atmosphere that may have exacerbated the heatwave.

To better establish the linkages between soil moisture and temperature extremes over Europe, we have applied the segmented regression analysis described in Section 3 to the ERA5 soil moisture and maximum temperature data across northern Europe for the 1979-2018 period to estimate a climatology of breakpoint statistics. Monthly results are shown in Figure 6. The estimated breakpoint between two linear regressions is only shown where the criteria outlined in Section 3 are met. Of all the grid cells in the domain, the number shaded rises from 51% in May to nearly 70% in July. The segmented regression calculation fails to converge for between 1-2% of cells, and only 2-3% of cells fail to pass the significance test even with the degrees of freedom reduced in proportion to the soil moisture memory timescale. The most common criterion to be failed is that the change in slope is not more negative on the dry side of the breakpoint – this happens for 45% of land grid cells in May, dropping to under 28% in July.

Despite passing these criteria, many points do not conform to our process-based expectation for soil moisture control of temperature in moisture-limited, energy-abundant situations. The breakpoint is shown both in units of volumetric soil moisture (Figure 6 left column) and as a normalized 0-1 index whose range is bounded by the lowest and highest daily soil moisture values registered in 40 years of ERA data for the month (middle column). It is clear from the index values that breakpoints in the higher range of local soil moisture (bluer colors) correspond with smaller changes in slope (yellower colors in the right column). This situation is persistent over much of Scandinavia and the British Isles, indicating that extremely warm and dry conditions are too rare to influence detection of a breakpoint toward the dry end of the range. In fact, the widespread areas of wet breakpoints paired with large slope changes over northern Scandinavia during May are associated with snowmelt and thawing ground within a moist, energy-limited environment rather than a heatwave feedback process. On the other hand, dry values for breakpoints paired with major changes in slope are common in all months across most of southern Europe and emerge in parts of the Northern European Plain and Eastern Europe during July and August. The large change in slope is indicative of a hypersensitive realm at very low soil moistures where daytime temperatures can elevate markedly as soil dries.

The relationship among the soil moisture breakpoint, change in slope $\frac{dT_{Max}}{dSM}$, surface fluxes and the strength of land-atmosphere coupling can be seen clearly in Figure 7. The correlation between latent heat flux and soil moisture is the main component of the terrestrial coupling index (Dirmeyer 2011), indicating strength of feedback of land surface states onto the lower troposphere. The L-shaped distribution in the left panel shows that strong coupling is associated with locations where the breakpoint occurs at relatively dry soil moisture. These also tend to be locations with abundant sensible heat flux, mostly in Southern Europe (right panel), indicative of a shutdown of evapotranspiration consistent with the theory described earlier. Locations with very low sensible heat flux, regardless of the estimated value of the breakpoint, have weak correlation or anti-correlation between latent heat flux and soil moisture, indicating that they are not moisture-limited locations where soil moisture content typically regulates surface flux partitioning. The breakpoint algorithm almost always finds a statistically significant change in slope, given such a large sample size, but often over Europe it is not indicative of a physical mechanism whereby the land surface control of atmospheric states is enhanced in dry conditions.

To attempt to verify the bivariate relationships related to land-atmosphere coupling shown so far using ERA5 data, we focus on Britain due to the availability of *in situ* soil moisture, meteorological and flux data. If we find that the observed relationships between links in the process chain of land-atmosphere coupling (Santanello et al., 2018) are represented well in ERA5 over Britain, we may use the reanalyses to extrapolate conclusions to the rest of northern Europe with greater confidence.

Figure 8 provides a diurnal Hovmöller diagram of the vertical profile of diabatic heating from ERA5, averaged over the land grid cells of the Britain box shown in Figure 3. The mean warm-season diurnal profile for the 39 years prior to 2018 shows the warming and deepening of the boundary layer from sunrise through the afternoon, with shallow cooling at night. Climatologically, there is convective warming that breaks through the boundary layer in the late afternoon, leading to enhanced mid-tropospheric warming due to latent heat release. In fact, there is weal warming in the mid-troposphere at all times of day due to frequent clouds. Climatologically the boundary layer height is above the lifted condensation level (LCL), another indication that Britain is more often cloudy than not. Peak surface sensible heat flux occurs an hour after noon at just over 100 Wm^{-2}. In 2018 daytime boundary layer heating is stronger during the day and cooling is weaker at night. There is less heating of the troposphere above the boundary layer due to less latent heat release from reduced cloudiness. There is actually net cooling above the boundary layer from mid-morning to mid-afternoon due to entrainment of lower potential temperature air from below becoming dominant given the lack of cloud formation. The LCL is higher while boundary layer depth is lower, and surface sensible heat flux is about 20% greater. Figure S4 presents a similar analysis for moisture fluxes – the anomalies at 08 and 20 UTC are artifacts of the data assimilation cycle, but otherwise more aggressive heating of the boundary layer appears to lead to stronger moisture diffusion and entrainment into the free atmosphere without condensation, but stronger nighttime drying of the lower troposphere and little change in surface latent heat flux.

Breakpoint analyses in the manner of Figure 2 are shown in Figure 9 for ten COSMOS-UK sites that have complete soil moisture and meteorological data for the summers of 2017 and 2018. The heatwave year of 2018 (red) shows a significant regression slope on the dry side of the breakpoint at every station that is steeper than on the wet side of the breakpoint, and in better agreement with the two-year estimate (green) than is the 2017 regression (blue). The soil moisture breakpoint values for 2018 are also more stable and in better agreement with the 2-year estimate than are the 2017-based values. 2017 slopes are often not significant and for several stations do not conform to the theory of dry soils driving higher temperature, likely because the 2017 sample does not contain many or any hot dry days typical of a land-atmosphere feedback. Figure 10 shows the same analysis for the ERA5 grid cells containing the COSMOS-UK sites. ERA5 estimates consistently show a shallower slope on the dry side of the breakpoint, indicating less sensitivity of daily maximum temperatures to drying soils than observations, and less of a change in slope (sensitivity) between the wet and dry sides of the breakpoint. The breakpoint algorithm struggles to find significant changes at some locations, like Hartwood Home and Riseholme where there is a clear signal in 2018 for the COSMOS-UK data but for neither year in ERA5. Overall it appears that ERA5 underestimates the impact of very dry soils on extreme temperatures, at least over Britain. A reason for the lower coupling to drought/Tmax in ERA5 might be the lack of soil moisture-vegetation feedback, since ERA5 adopts a monthly climatology of leaf area index (Boussetta et al., 2013). Moreover, recent findings by Nogueira et al. (2020) highlight the interplay of vegetation cover and state in further enhancing surface temperatures.

Figure S5 compares the results from Figures 9 and 10 for four categories of breakpoint statistics. Compared to the ten COSMOS sites, ERA5 consistently overestimates the volumetric soil water content at the breakpoint, underestimates the sensitivity of daily maximum temperature to drying soils, and overestimates the correlation between maximum temperature and soil moisture on the dry side of the breakpoint. ERA5 also gives a very uniform difference between 2018 and 2017, showing 30-45% more dry days in 2018, while COSMOS observations show a wider range from 10-56% increases for 2018. Most of these discrepancies could be explained by the differing natures of point measurements versus model grid cell estimates. Model data contains no observational error, so the higher regression correlations for ERA5 are to be expected as there is no random error to degrade correlations. Reduced sensitivity in ERA5 may be attributed to the large spatial area of a model grid cell, nearly 10^3 km^2, muting variability and causing all of the blue linear-fit lines to be flatter than the 1:1 red dotted line. This may also explain the uniformity in the difference between 2018 and 2017 dry days, as local variations in rainfall and hillslope properties that affect local soil moisture are not resolved in ERA5. However, the systematic overestimation by ERA5 of soil water content at the breakpoint suggests a bias in model soil parameters or perhaps model physics. The only significant inter-station correlation found between ERA5 and COSMOS is for the magnitude of the correlation on the dry side of the breakpoint (shown in green), although all are positively correlated.

There are fewer flux towers than COSMOS-UK sites that have data necessary to assess breakpoint relationships between surface fluxes and soil moisture. The Great Fen site has time domain transmissometry (TDT) soil moisture sensors only (surface layer data are used), while Sheepdrove is also a COSMOS-UK site. Breakpoint analysis of evaporative fraction (EF) versus volumetric soil water content for these stations is shown in Figure 11; Figures S6 and S7 show results separately for sensible and latent heat fluxes. At Sheepdrove, the soil moisture breakpoints estimated independently using EF and maximum air temperature (Figure 11) are within 1% of each other for the two years combined, suggesting a mechanistic link between soil moisture and extreme temperature via surface heat flux partitioning. As with previous figures, the flux-based results are less representative and robust for 2017, although at Great Fen there are significant dry-side sensitivities for both years that are very similar to each other.

The same analysis with ERA5 (right panels) differs systematically from the flux tower analysis. In ERA5, there appears to be too much sensitivity of EF to soil moisture variations when soils are wet (greater positive slope). The field sites show EF values consistently centering on 0.8 on the wet side of the breakpoint, whereas ERA5 ranges from 0.9 down to 0.7 at the breakpoint. ERA5 also shows much less sensitivity on the dry side of the breakpoint (compare slope values in the green boxes). In other words, the break is much clearer in observations than the reanalysis. ERA5 grid cells represent an area average, so it may actually characterize the net distribution of heterogeneous drydowns and their effect on fluxes rather well. That cannot be discerned from this analysis, but this comparison to point data at flux towers shows stark differences. At both sites during the drought, EF attains lower daily values of EF than does ERA5. Examination of sensible and latent heat fluxes separately (Figures S6 and S7) show that in all cases, most of the signal in evaporative fraction comes from the sensible heat flux, and the contrast in distributions on either side of the estimated breakpoints is always starker in observations than in ERA5. Nevertheless, ERA5 does reproduce the overall signature of increasing sensitivity of surface fluxes to soil moisture as soils dry below a critical point.

Some of the COSMOS-UK sites have eddy covariance estimates of sensible heat flux and the necessary radiation and ground heat flux measurements to estimate latent heat flux as a residual for 2017 and 2018. The estimated breakpoints for sensible heat flux and EF at those six sites are shown in Figure 12. At every site, there is a significant detection of a breakpoint for sensible heat flux and significantly sharper increases over drier soils. For evaporative fraction, the relationships are slightly less clear, consistent with the weaker role of soil moisture controls on latent heat flux suggested in Figures S6, S7 and 11. Although not apparent to the eye, the change in slope for EF at Redhill is significant but the position of the breakpoint is unreliable, indicated by the grey oval of uncertainty. Porton Down is similarly uncertain for EF, and the change in slope across the breakpoint is not of the expected sign. However, in each case, the correlation of the linear regression on the dry side of the breakpoint is stronger than on the wet side, suggesting increased control of soil moisture over surface fluxes as drought sets in. Furthermore, the values of volumetric soil water content of the breakpoints calculated at each station using either EF, sensible heat flux or evaporative fraction are much closer together than are the average breakpoint values among stations. This is true for in situ data and ERA5 grid cells containing the stations. 91% of the total variance in breakpoint soil moisture values in observations is due to inter-station variance; for ERA5 data it is 86%. The remaining variance is the small disagreements between estimates using maximum temperature or different surface fluxes. Furthermore, at every location for every variable in either source of data, the correlation of the linear regression on the dry side of the breakpoint is greater and more significant than on the wet side. All these results suggest a real physical link between declining soil moisture, flux anomalies and extreme heat.

The comparison of ERA5 to field observations over Britain provides context to interpret continental maps of drought – heatwave breakpoint statistics. We find that just as with Figure 6, European maps of EF breakpoint statistics are quite stable from month to month (Figure S8) and the spatial patterns of breakpoints are very consistent between EF and maximum temperature. Table 1 shows the degree to which soil moisture breakpoint values calculated with surface fluxes from ERA5 agree with maximum temperature-based breakpoint estimates. Differences are quite small between breakpoints estimated with any variable except latent heat flux, which shows a strong positive bias (breakpoint occurring at a higher value of soil water content) and root mean square errors 15-45% higher than other flux variables. The relationship between soil water content and sensible heat flux appears to be the controlling factor for temperature sensitivity amplification during combined drought heatwave cases, supporting in a temporal sense the result suggested spatially in Figure 7.

Finally, the fraction of days during May through August 2018 that lie on the dry side of the climatologically estimate breakpoints based on both maximum temperature and evaporative fraction are shown in Figure 13. In each case, the climatological fraction of days is subtracted, so that positive values suggest more days than average in the hypersensitive soil moisture regime during 2018. Comparison to Figure 3 shows how this metric synthesizes the extremes in soil water content and temperature, as well as providing a spatial depiction of regions where land-atmosphere feedbacks could have exacerbated the hot conditions in 2018. Large portions of northern Europe experienced at least a 25% increase in the number of critically dry soil days, including not only the three regions highlighted earlier in the study, but also over large areas of the eastern Baltic and western Eurasian steppes. Very few areas had a decrease in the number of critically dry days during the warm season of 2018.

5. Conclusions

In this study, we have used a combination of high-quality reanalyses and *in situ* measurements of volumetric soil water content, temperature and surface fluxes to demonstrate the existence of a breakpoint in the range of soil water content below which the sensitivity of the atmosphere to drying soils substantially increases, providing a potential positive feedback mechanism by which the land surface may exacerbate heatwaves during drought conditions. Specifically, we diagnose the 2018 drought and heatwave over Northern Europe, an area that rarely enters into classically defined regimes amenable to land-atmosphere feedbacks (Santanello et al., 2018; Seneviratne et al., 2010).

During 2018, exceptionally dry conditions spread throughout much of northern Europe in concurrence with multiple prolonged episodes of extreme heat. Segmented regression analysis uninformed by any physical processes has been found to identify stable values of breakpoints in the range of soil water content consistently at most locations, including soil moisture monitoring sites in Britain. The values of soil water content are largely invariant from month to month when calculated on a monthly basis and are also very similar whether the regressions are trained with dependent variable being daily maximum air temperature, sensible heat flux or evaporative fraction. There are greater variations when latent heat flux is the dependent variable, suggesting the loss of evaporative cooling is less of a regulator of extreme heat than the direct warming of desiccated land surfaces and transfer of that heat to the atmosphere.

Patterns over Europe in ERA5 data show very broad potential for land-atmosphere feedbacks to have exacerbated the extreme heat during 2018. However, field data over Britain suggest ERA5 may underestimate the increase of sensitivity of extreme temperatures to declining soil moisture in very dry conditions, so the European maps based on ERA5 data may not represent the full potential impact of drying soils on heatwaves. The present study cannot establish the degree to which scale differences between the flux tower and COSMOS soil moisture sites (with a footprint no larger than 1 km^2) and ERA5 grid cells (around 10^3 km^2) contribute to the discrepancies. Few areas of Europe were free from dry conditions during the summer of 2018, so a combination of local land-driven feedback mechanisms suggested here and non-local mechanisms (Berg et al., 2016; Miralles et al., 2018; Schumacher et al., 2019) could have contributed to the observed extremes.

The consistency of apparent breakpoint thresholds of soil moisture below which surface fluxes and daily maximum temperatures become hypersensitive to declining soil moisture provides a source of predictability for severe heatwaves. Recognition of the role of low soil moisture in exacerbating extreme heat, the correct representation in forecast models of the processes governing the increased sensitivity, and proper initialization of those forecast models with real-time soil moisture conditions will all contribute to increased forecast skill and improved early warning of heatwaves, even in regions which have historically been immune from such extremes.

Acknowledgements:

This research is the result of Dr. Dirmeyer's sabbatical visits to the European Centre for Medium-range Weather Forecasts in July 2018 and March-April 2019, hosted by Dr. Balsamo. A portion of this work was supported by the Natural Environment Research Council award number NE/R016429/1 as part of the UK-SCAPE programme delivering National Capability. UKCEH field data are available as indicated through the references provided herein to the Centre's online data catalogue (see: https://catalogue.ceh.ac.uk/eidc/documents). The Copernicus Climate Change

Service (C3S) provides access to ERA5 data freely through its online portal at: https://cds.climate.copernicus.eu/cdsapp#!/home.

References

Albergel, C., Dorigo, W., Reichle, R. H., Balsamo, G., de Rosnay, P., Muñoz-Sabater, J., et al. (2013). Skill and Global Trend Analysis of Soil Moisture from Reanalyses and Microwave Remote Sensing. *Journal of Hydrometeorology*, *14*(4), 1259–1277. https://doi.org/10.1175/JHM-D-12-0161.1

Albergel, Clément, Dutra, E., Bonan, B., Zheng, Y., Munier, S., Balsamo, G., et al. (2019). Monitoring and Forecasting the Impact of the 2018 Summer Heatwave on Vegetation. *Remote Sensing*, *11*(5), 520. https://doi.org/10.3390/rs11050520

Antoniou, V., Askquith-Ellis, A., Bagnoli, S., Ball, L., Bennett, E., Blake, J., et al. (2019, August 19). COSMOS-UK user guide: users' guide to sites, instruments and available data (version 2.10) [Publication - Report]. Retrieved May 18, 2020, from https://cosmos.ceh.ac.uk/sites/default/files/COSMOS-UK%20User%20Guide%20v2.10.pdf

Berg, A., Findell, K., Lintner, B., Giannini, A., Seneviratne, S. I., Hurk, B. van den, et al. (2016). Land–atmosphere feedbacks amplify aridity increase over land under global warming. *Nature Climate Change*, *6*(9), 869–874. https://doi.org/10.1038/nclimate3029

Betts, A. K. (2004). Understanding Hydrometeorology Using Global Models. *Bulletin of the American Meteorological Society*, *85*(11), 1673–1688. https://doi.org/10.1175/BAMS-85-11-1673

Boussetta, S., Balsamo, G., Beljaars, A., Kral, T., & Jarlan, L. (2013). Impact of a satellite-derived leaf area index monthly climatology in a global numerical weather prediction model. *International Journal of Remote Sensing*, *34*(9–10), 3520–3542. https://doi.org/10.1080/01431161.2012.716543

Casanueva, A., Burgstall, A., Kotlarski, S., Messeri, A., Morabito, M., Flouris, A. D., et al. (2019). Overview of Existing Heat-Health Warning Systems in Europe. *International Journal of Environmental Research and Public Health*, *16*(15), 2657. https://doi.org/10.3390/ijerph16152657

Crowhurst, D., Morrison, R., Evans, J., Cooper, H., Cumming, A., Fry, M., & Boorman, D. (2019, September). *Actual evaporation data system for COSMOS-UK*. Workshop presented at the Hydro-JULES: Next Generation Land Surface and Hydrological Predictions, The Royal Society, London. Retrieved from http://nora.nerc.ac.uk/id/eprint/525105/

Dirmeyer, P. A., Schlosser, C. A., & Brubaker, K. L. (2009). Precipitation, Recycling, and Land Memory: An Integrated Analysis. *Journal of Hydrometeorology*, *10*(1), 278–288. https://doi.org/10.1175/2008JHM1016.1

Dirmeyer, P. A., Balsamo, G., & Peters-Lidard, C. D. (2015). Land-Atmosphere Interactions and the Water Cycle. In *Seamless Prediction of the Earth System: from Minutes to Months (G Brunet, S Jones, PM Ruti Eds.)* (pp. 145–154). Geneva, Switzerland: World Meteorological Organization.

Dirmeyer, P. A., Gentine, P., Ek, M. B., & Balsamo, G. (2018). Land Surface Processes Relevant to S2S Prediction. In *The Gap Between Weather and Climate Forecasting: Sub-Seasonal to Seasonal Prediction* (Vol. A. W. Robertson and F. Vitart Eds., pp. 166–182). Elsevier.

Dirmeyer, P. A., Chen, L., Wu, J., Shin, C.-S., Huang, B., Cash, B. A., et al. (2018). Verification of Land–Atmosphere Coupling in Forecast Models, Reanalyses, and Land Surface Models Using Flux Site Observations. *Journal of Hydrometeorology*, *19*(2), 375–392. https://doi.org/10.1175/JHM-D-17-0152.1

Ek, M. B., & Holtslag, A. a. M. (2004). Influence of Soil Moisture on Boundary Layer Cloud Development. *Journal of Hydrometeorology*, *5*(1), 86–99. https://doi.org/10.1175/1525-7541(2004)005<0086:IOSMOB>2.0.CO;2

Evans, J. G., Ward, H. C., Blake, J. R., Hewitt, E. J., Morrison, R., Fry, M., et al. (2016). Soil water content in southern England derived from a cosmic-ray soil moisture observing system – COSMOS-UK. *Hydrological Processes*, *30*(26), 4987–4999. https://doi.org/10.1002/hyp.10929

Fischer, E. M., Seneviratne, S. I., Lüthi, D., & Schär, C. (2007). Contribution of land-atmosphere coupling to recent European summer heat waves. *Geophysical Research Letters*, *34*(6). https://doi.org/10.1029/2006GL029068

Fratini, G., & Mauder, M. (2014). Towards a consistent eddy-covariance processing: an intercomparison of EddyPro and TK3. *Atmospheric Measurement Techniques*, *7*(7), 2273–2281. https://doi.org/10.5194/amt-7-2273-2014

Gentine, P., Holtslag, A. A. M., D'Andrea, F., & Ek, M. (2013). Surface and Atmospheric Controls on the Onset of Moist Convection over Land. *Journal of Hydrometeorology*, *14*(5), 1443–1462. https://doi.org/10.1175/JHM-D-12-0137.1

Hersbach, H., Bell, B., Berrisford, P., Hirahara, S., Horányi, A., Muñoz-Sabater, J., et al. (2020). The ERA5 Global Reanalysis. *Quarterly Journal of the Royal Meteorological Society*, (accepted). https://doi.org/10.1002/qj.3803

Hirsch, A. L., Pitman, A. J., Seneviratne, S. I., Evans, J. P., & Haverd, V. (2014). Summertime maximum and minimum temperature coupling asymmetry over Australia determined using WRF. *Geophysical Research Letters*, *41*(5), 1546–1552. https://doi.org/10.1002/2013GL059055

Horst, S. V. J. van der, Pitman, A. J., Kauwe, M. G. D., Ukkola, A., Abramowitz, G., & Isaac, P. (2019). How representative are FLUXNET measurements of surface fluxes during temperature extremes? *Biogeosciences*, *16*(8), 1829–1844. https://doi.org/10.5194/bg-16-1829-2019

Kendon, M., McCarthy, M., Jevrejeva, S., Matthews, A., & Legg, T. (2019). State of the UK climate 2018. *International Journal of Climatology*, *39*(S1), 1–55. https://doi.org/10.1002/joc.6213

Kornhuber, K., Osprey, S., Coumou, D., Petri, S., Petoukhov, V., Rahmstorf, S., & Gray, L. (2019). Extreme weather events in early summer 2018 connected by a recurrent hemispheric wave-7 pattern. *Environmental Research Letters*, *14*(5), 054002. https://doi.org/10.1088/1748-9326/ab13bf

Koster, R. D., Sud, Y. C., Guo, Z., Dirmeyer, P. A., Bonan, G., Oleson, K. W., et al. (2006). GLACE: The Global Land–Atmosphere Coupling Experiment. Part I: Overview. *Journal of Hydrometeorology*, *7*(4), 590–610. https://doi.org/10.1175/JHM510.1

Lass, W., Haas, A., Hinkel, J., & Jaeger, C. (2011). Avoiding the avoidable: Towards a European heat waves risk governance. *International Journal of Disaster Risk Science*, *2*(1), 1–14. https://doi.org/10.1007/s13753-011-0001-z

Lau, N.-C., & Nath, M. J. (2014). Model Simulation and Projection of European Heat Waves in Present-Day and Future Climates. *Journal of Climate*, *27*(10), 3713–3730. https://doi.org/10.1175/JCLI-D-13-00284.1

Magnusson, L., Ferranti, L., & Vamborg, F. (2018). Forecasting the 2018 European heatwave. *ECMWF Newsletter*, *157*, 2–3.

Miralles, D. G., Gentine, P., Seneviratne, S. I., & Teuling, A. J. (2018). Land–atmospheric feedbacks during droughts and heatwaves: state of the science and current challenges. *Annals of the New York Academy of Sciences*, *0*(0), 1–17. https://doi.org/10.1111/nyas.13912

Morrison, R., Cooper, H., Cumming, A., Scarlett, P., Thornton, J., & Winterbourn, B. (2019). Eddy covariance measurements of carbon dioxide, energy and water fluxes at an organically managed grassland, Berkshire, UK, 2017 to 2019. Retrieved May 18, 2020, from https://catalogue.ceh.ac.uk/id/5a93161f-0124-4650-a2c9-7e8aaea7e6bb

Morrison, R., Cooper, H., Cumming, A., Evans, C., Thomton, J., Winterbourn, B., et al. (2020). Eddy covariance measurements of carbon dioxide, energy and water fluxes at a cropland and a grassland on lowland peat soils, East Anglia, UK, 2016-2019. Retrieved May 18, 2020, from https://catalogue.ceh.ac.uk/id/2fe84b80-117a-4b19-a1f5-71bbd1dba9c9

Muggeo, V. M., & Hajat, S. (2009). Modelling the non-linear multiple-lag effects of ambient temperature on mortality in Santiago and Palermo: a constrained segmented distributed lag approach. *Occupational and Environmental Medicine*, *66*(9), 584–591. https://doi.org/10.1136/oem.2007.038653

Muggeo, V. M. R. (2003). Estimating regression models with unknown break-points. *Statistics in Medicine*, *22*(19), 3055–3071. https://doi.org/10.1002/sim.1545

Nogueira, M., Albergel, C., Boussetta, S., Johannsen, F., Trigo, I. F., Ermida, S. L., et al. (2020). Role of vegetation in representing land surface temperature in the CHTESSEL (CY45R1) and SURFEX-ISBA (v8.1) land surface models: a case study over Iberia. *Geoscientific Model Development Discussions*, 1–29. https://doi.org/10.5194/gmd-2020-49

Papale, D., Reichstein, M., Aubinet, M., Canfora, E., Bernhofer, C., Kutsch, W., et al. (2006). Towards a standardized processing of Net Ecosystem Exchange measured with eddy covariance technique: algorithms and uncertainty estimation. *Biogeosciences*, *3*(4), 571–583. https://doi.org/10.5194/bg-3-571-2006

Petch, J. C., Short, C. J., Best, M. J., McCarthy, M., Lewis, H. W., Vosper, S. B., & Weeks, M. (2020). Sensitivity of the 2018 UK summer heatwave to local sea temperatures and soil moisture. *Atmospheric Science Letters*, *21*(3), e948. https://doi.org/10.1002/asl.948

Philip, S. Y., Kew, S. F., Hauser, M., Guillod, B. P., Teuling, A. J., Whan, K., et al. (2018). Western US high June 2015 temperatures and their relation to global warming and soil moisture. *Climate Dynamics*, *50*(7–8), 2587–2601. https://doi.org/10.1007/s00382-017-3759-x

Reichstein, M., Falge, E., Baldocchi, D., Papale, D., Aubinet, M., Berbigier, P., et al. (2005). On the separation of net ecosystem exchange into assimilation and ecosystem respiration: review and improved algorithm. *Global Change Biology*, *11*(9), 1424–1439. https://doi.org/10.1111/j.1365-2486.2005.001002.x de Rosnay, P., Balsamo, G., Albergel, C., Muñoz-Sabater, J., & Isaksen, L. (2014). Initialisation of Land Surface Variables for Numerical Weather Prediction. *Surveys in Geophysics*, *35*(3), 607–621. https://doi.org/10.1007/s10712-012-9207-x

Rösner, B., Benedict, I., van Heerwaarden, C., Weerts, A., Hazeleger, W., Bissolli, P., & Trachte, K. (2019). The long heat wave and drought in Europe in 2018. *Bulletin of the American Meteorological Society*, *100*(9), S222–S223. https://doi.org/10.1175/2019BAMSStateoftheClimate.1

Rosolem, R., Shuttleworth, W. J., Zreda, M., Franz, T. E., Zeng, X., & Kurc, S. A. (2013). The Effect of Atmospheric Water Vapor on Neutron Count in the Cosmic-Ray Soil Moisture Observing System. *Journal of Hydrometeorology*, *14*(5), 1659–1671. https://doi.org/10.1175/JHM-D-12-0120.1

Russo, S., Sillmann, J., & Fischer, E. M. (2015). Top ten European heatwaves since 1950 and their occurrence in the coming decades. *Environmental Research Letters*, *10*(12), 124003. https://doi.org/10.1088/1748-9326/10/12/124003

Samaniego, L., Thober, S., Kumar, R., Wanders, N., Rakovec, O., Pan, M., et al. (2018). Anthropogenic warming exacerbates European soil moisture droughts. *Nature Climate Change*, *8*(5), 421–426. https://doi.org/10.1038/s41558-018-0138-5

Santanello, J. A., Friedl, M. A., & Ek, M. B. (2007). Convective Planetary Boundary Layer Interactions with the Land Surface at Diurnal Time Scales: Diagnostics and Feedbacks. *Journal of Hydrometeorology*, *8*(5), 1082–1097. https://doi.org/10.1175/JHM614.1

Santanello, J. A., Peters-Lidard, C. D., Kumar, S. V., Alonge, C., & Tao, W.-K. (2009). A Modeling and Observational Framework for Diagnosing Local Land–Atmosphere Coupling on Diurnal Time Scales. *Journal of Hydrometeorology*, *10*(3), 577–599. https://doi.org/10.1175/2009JHM1066.1

Santanello, J. A., Peters-Lidard, C. D., & Kumar, S. V. (2011). Diagnosing the Sensitivity of Local Land–Atmosphere Coupling via the Soil Moisture–Boundary Layer Interaction. *Journal of Hydrometeorology*, *12*(5), 766–786. https://doi.org/10.1175/JHM-D-10-05014.1

Santanello, J. A., Dirmeyer, P. A., Ferguson, C. R., Findell, K. L., Tawfik, A. B., Berg, A., et al. (2018). Land-Atmosphere Interactions: The LoCo Perspective. *Bulletin of the American Meteorological Society*, *99*, 1253–1272. https://doi.org/10.1175/BAMS-D-17-0001.1

Schumacher, D. L., Keune, J., Heerwaarden, C. C. van, Arellano, J. V.-G. de, Teuling, A. J., & Miralles, D. G. (2019). Amplification of mega-heatwaves through heat torrents fuelled by upwind drought. *Nature Geoscience*, *12*(9), 712–717. https://doi.org/10.1038/s41561-019-0431-6

Schwingshackl, C., Hirschi, M., & Seneviratne, S. I. (2018). A theoretical approach to assess soil moisture–climate coupling across CMIP5 and GLACE-CMIP5 experiments. *Earth System Dynamics*, *9*(4), 1217–1234. https://doi.org/10.5194/esd-9-1217-2018

Seneviratne, S. I., Lüthi, D., Litschi, M., & Schär, C. (2006). Land–atmosphere coupling and climate change in Europe. *Nature*, *443*(7108), 205–209. https://doi.org/10.1038/nature05095

Seneviratne, S. I., Corti, T., Davin, E. L., Hirschi, M., Jaeger, E. B., Lehner, I., et al. (2010). Investigating soil moisture–climate interactions in a changing climate: A review. *Earth-Science Reviews*, *99*(3), 125–161. https://doi.org/10.1016/j.earscirev.2010.02.004

Sousa, P. M., Barriopedro, D., Ramos, A. M., García-Herrera, R., Espírito-Santo, F., & Trigo, R. M. (2019). Saharan air intrusions as a relevant mechanism for Iberian heatwaves: The record breaking events of August 2018 and June 2019. *Weather and Climate Extremes*, *26*, 100224. https://doi.org/10.1016/j.wace.2019.100224

Stanley, S., Antoniou, V., Ball, L. A., Bennett, E. S., Blake, J. R., Boorman, D. B., et al. (2019). Daily and sub-daily hydrometeorological and soil data (2013-2017) [COSMOS-UK]. Retrieved May 18, 2020, from https://catalogue.ceh.ac.uk/id/a6012796-291c-4fd6-a7ef-6f6ed0a6cfa5

Teuling, A. J. (2018). A hot future for European droughts. *Nature Climate Change*, *8*(5), 364–365. https://doi.org/10.1038/s41558-018-0154-5

Vicente-Serrano, S. M., Lopez-Moreno, J.-I., Beguería, S., Lorenzo-Lacruz, J., Sanchez-Lorenzo, A., García-Ruiz, J. M., et al. (2014). Evidence of increasing drought severity caused by temperature rise in southern Europe. *Environmental Research Letters*, *9*(4), 044001. https://doi.org/10.1088/1748-9326/9/4/044001

Wolf, S., Keenan, T. F., Fisher, J. B., Baldocchi, D. D., Desai, A. R., Richardson, A. D., et al. (2016). Warm spring reduced carbon cycle impact of the 2012 US summer drought. *Proceedings of the National Academy of Sciences*, *113*(21), 5880–5885. https://doi.org/10.1073/pnas.1519620113

Wu, J., & Dirmeyer, P. A. (2020). Drought Demise Attribution Over CONUS. *Journal of Geophysical Research: Atmospheres*, *125*(4), e2019JD031255. https://doi.org/10.1029/2019JD031255

Zhang, Y., Wang, L., Santanello, J. A., Pan, Z., Gao, Z., & Li, D. (2020). Aircraft observed diurnal variations of the planetary boundary layer under heat waves. *Atmospheric Research*, *235*, 104801. https://doi.org/10.1016/j.atmosres.2019.104801

Zscheischler, J., Westra, S., Hurk, B. J. J. M. van den, Seneviratne, S. I., Ward, P. J., Pitman, A., et al. (2018). Future climate risk from compound events. *Nature Climate Change*, *8*(6), 469–477. https://doi.org/10.1038/s41558-018-0156-3

Table 1. Mean difference and root mean square difference (RMSE) between volumetric soil moisture content values at breakpoint when estimated using daily maximum temperature (as in Figure 6) versus the indicated surface flux terms (EF = evaporative fraction, SH = sensible heat flux, LH = latent heat flux). The domain for calculations is as in Figure 6, units are m^3m^{-3}.

	Mean Difference			RMSE		
	EF	SH	LH	EF	SH	LH
May	0.008	0.001	0.028	0.061	0.049	0.063
June	0.007	-0.006	0.028	0.053	0.049	0.064
July	-0.003	0.011	0.041	0.054	0.048	0.074
August	-0.007	0.005	0.028	0.054	0.050	0.067

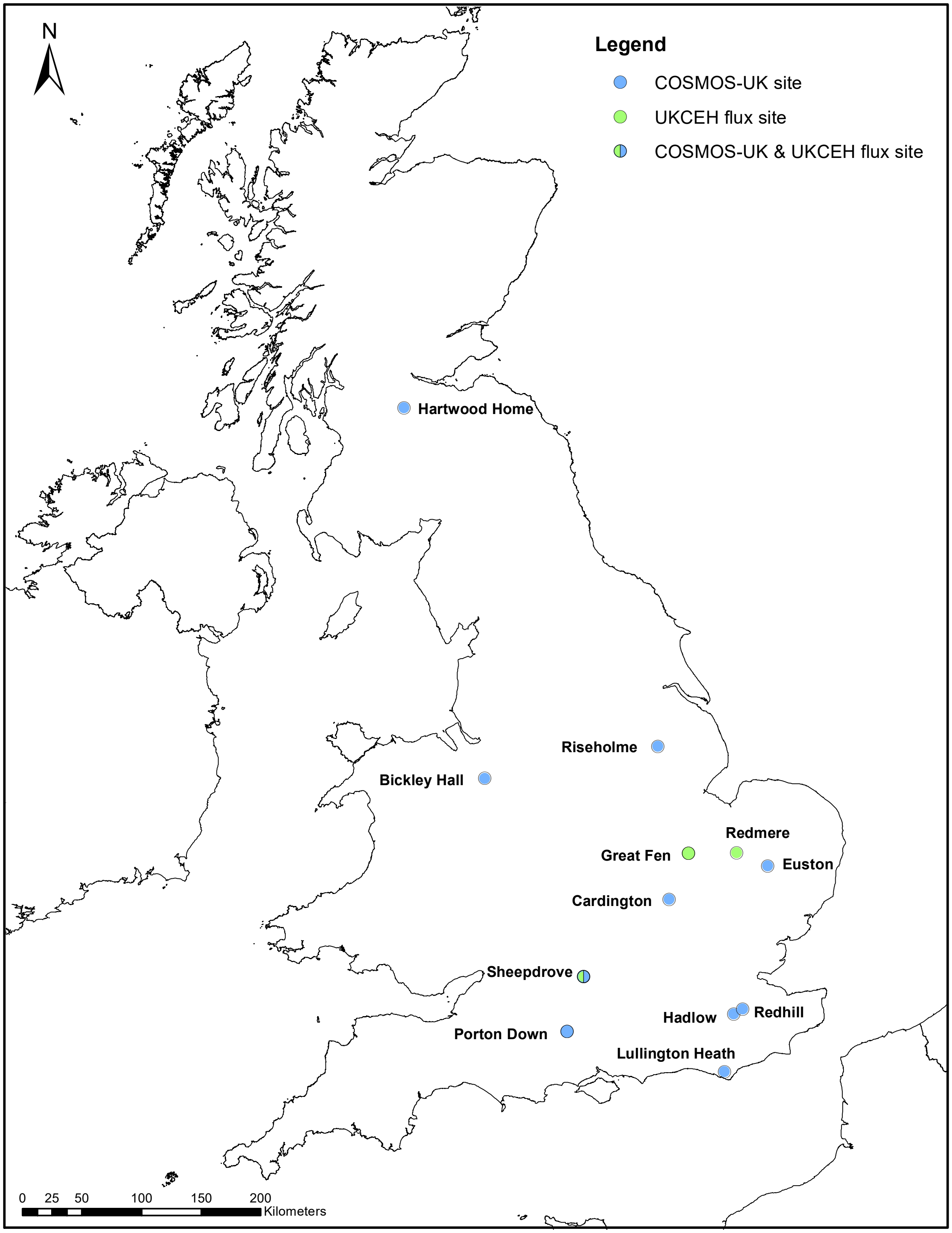

721 **Figure 1**. Locations of soil moisture and flux tower sites in Britain used in this study.

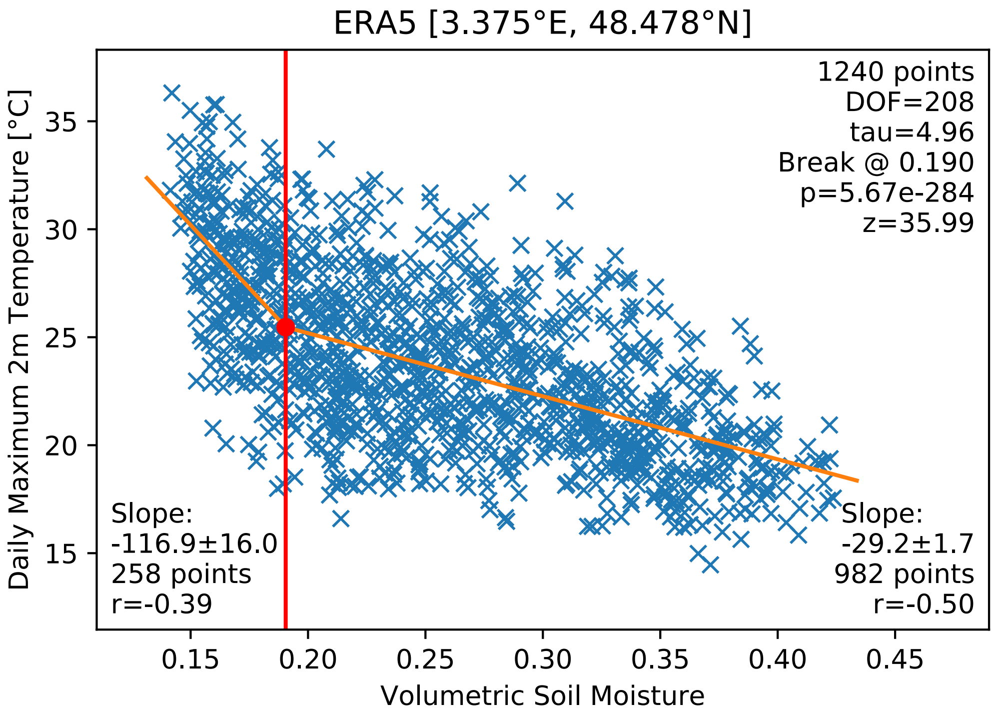

Figure 2: Relationship between daily maximum 2m air temperature (dependent variable; ordinate) and surface volumetric soil moisture (abscissa) during July for 1979-2018 at a grid cell in France. Values in upper right refer to the total number of days (including soil moisture memory time scale "tau" in days and reduced degrees of freedom "DOF" due to soil moisture autocorrelation) and significance of the estimate of the breakpoint between two best-fit linear regressions. Values in the lower corners show the estimated slopes, standard error of estimates, number of points and correlations for each segment – the fits for each segment are significant at the 99% confidence level.

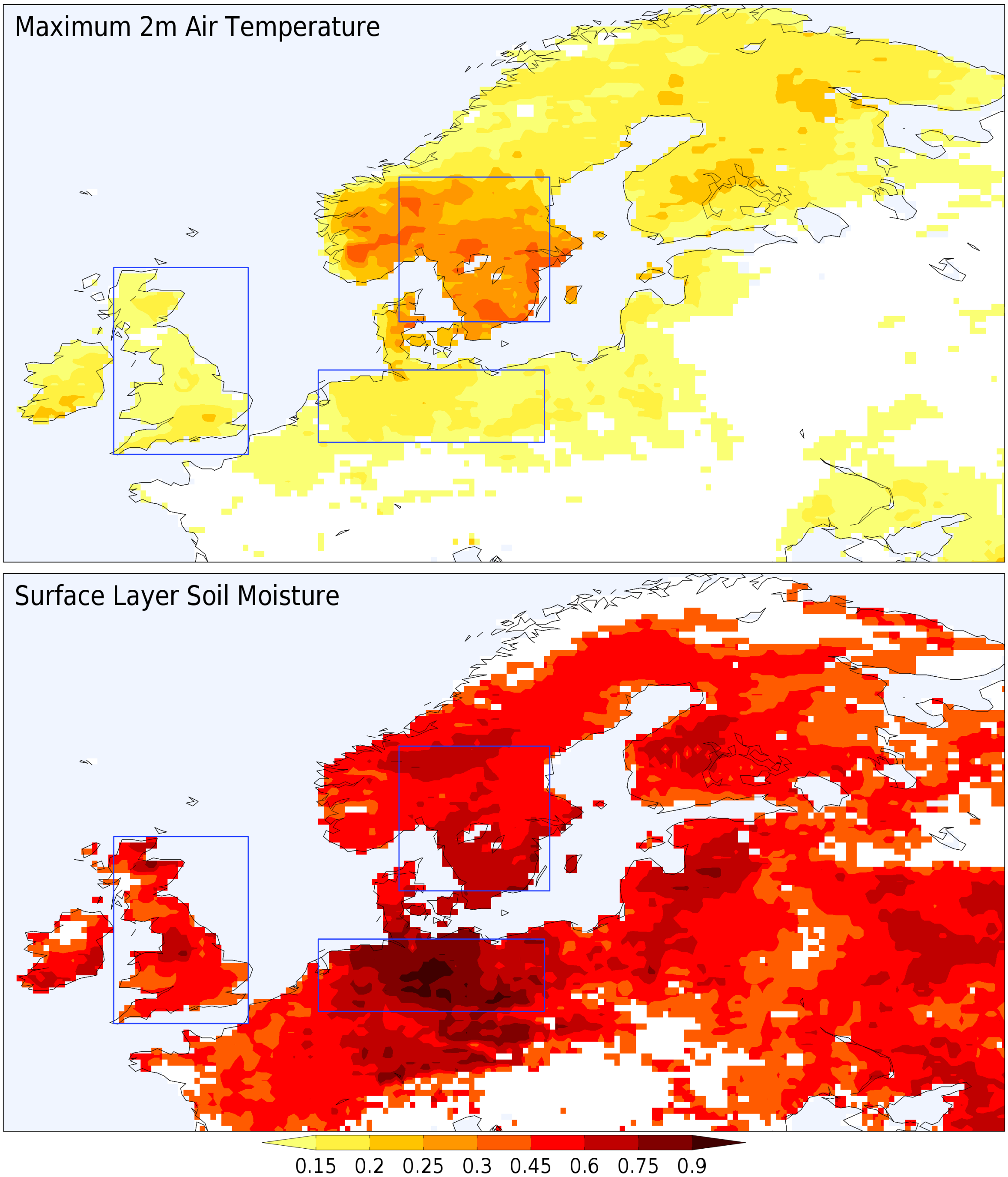

Figure 3: Fraction of days during May, June, July and August 2018 that are among 5% of warmest anomalies in maximum 2m air temperature (top); 25% driest absolute surface layer volumetric soil water content (bottom); compared to all days in May, June, July and August of 1979-2018. Colored areas are significant at the 99% confidence level. Blue boxes outline regions where land-only averages are shown in Figure 5.

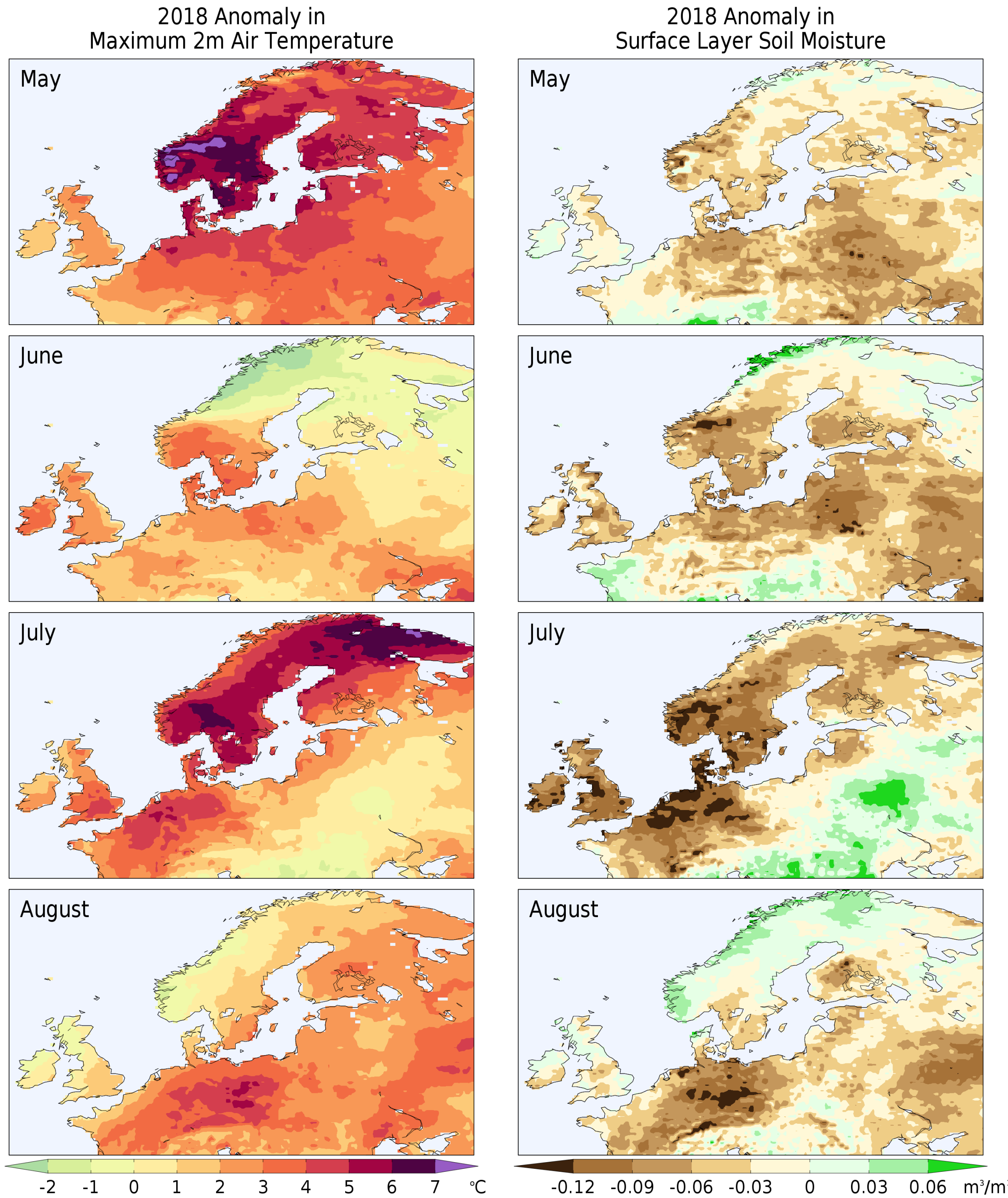

Figure 4: Monthly anomalies during 2018 in daily maximum 2m air temperature (left column) and surface volumetric soil water content (right column) in ERA5 compared to the 1979-2018 mean.

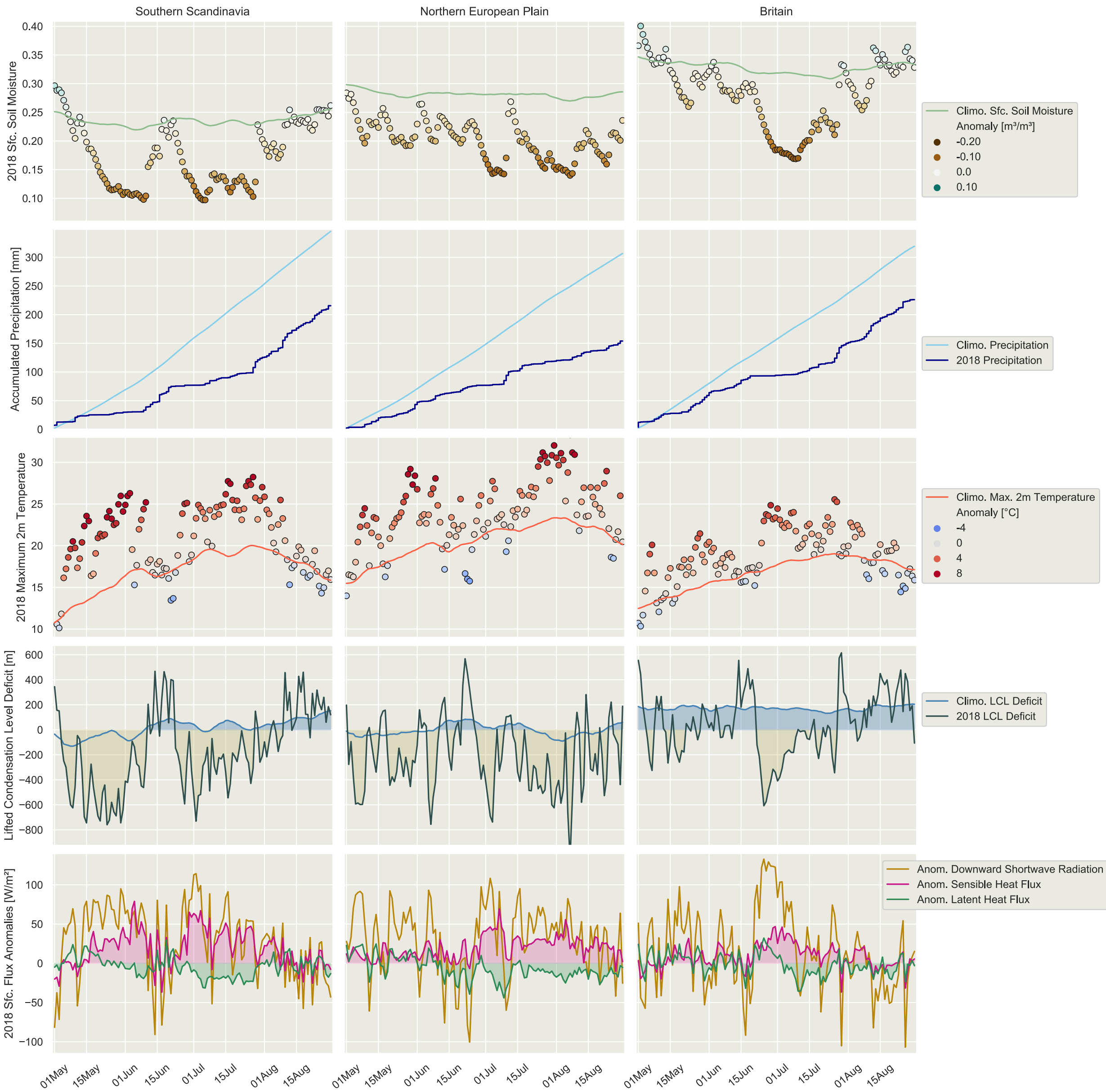

Figure 5: Area averages from ERA5 over the regions indicated in Figure 3 of daily surface layer volumetric soil water content (top row), cumulative precipitation (second row), daily maximum 2m air temperature (third row), LCL deficit (fourth row) and indicated surface energy balance terms (bottom row). In each panel, climatological values are indicated by a smooth (7-day centered running mean) line except in the bottom row where only anomalies are shown. In the first and third rows, color of dots indicates the magnitude of the anomaly.

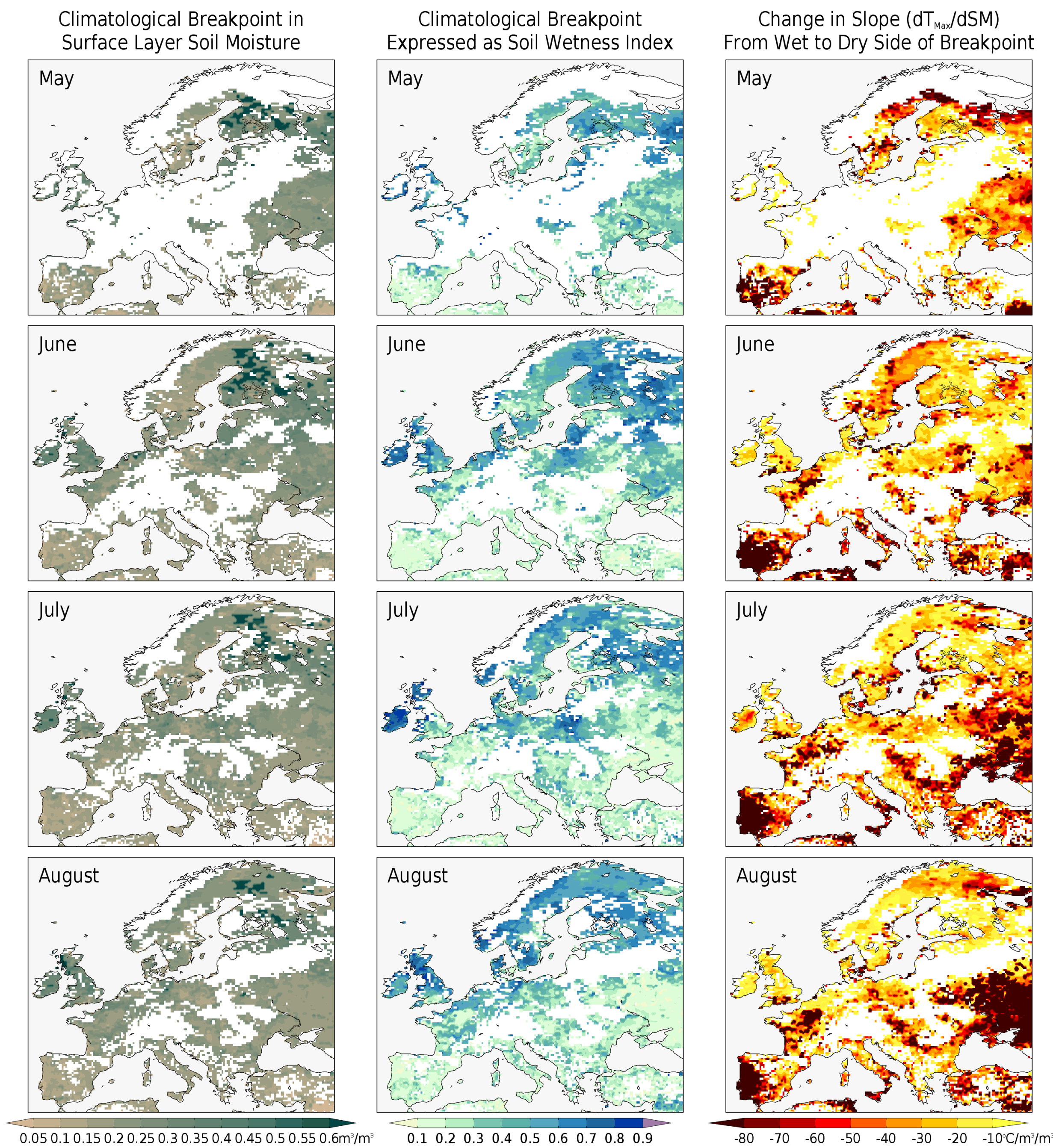

Figure 6: Values of volumetric soil water content (left column) and soil wetness index (middle column; see text for description) estimated to be at the breakpoint regarding a change in the slope of the regression of daily maximum 2m air temperature on soil water content. The right column shows the change in the slope of the regression. White areas fail to pass at least one of the criteria described in Section 3, with an additional criterion that the estimated value of the maximum temperature at the breakpoint exceed 10°C.

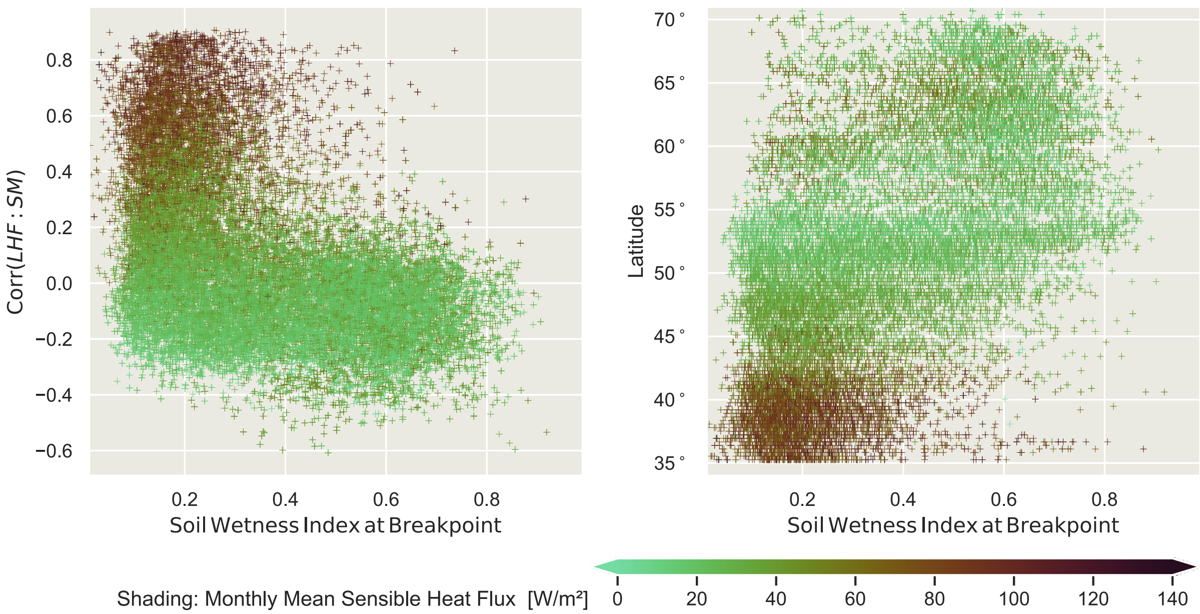

Figure 7: Scatter plots relating the estimated monthly breakpoint values of soil wetness index estimated for May, June, July and August to the temporal correlation between latent heat flux and soil moisture (left panel), latitude (right panel) and surface sensible heat flux (color in both panels) using ERA5 data. Each point is one land grid cell and one of the four months over the European domain shown in Figure 6; estimates use 40 years of data (1979-2018).

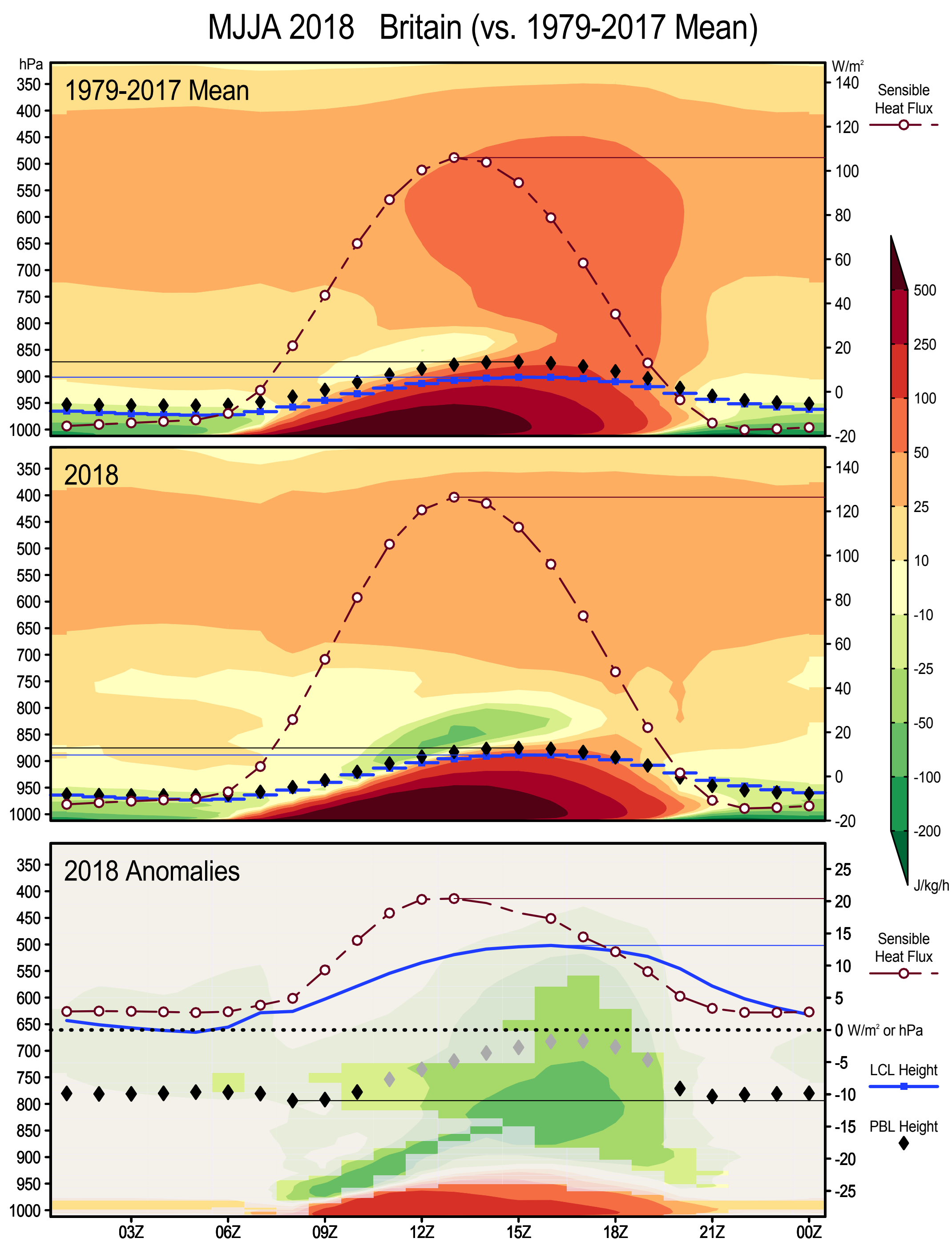

Figure 8: Time – height (model pseudo-pressure coordinate, scale on the left; see Section 2 for details) diagram of hourly heat budget terms averaged over land grid cells of Britain (see box in Figure 3) from ERA5 data. Shading is total diabatic heating per hour – insignificant anomalies for 2018 are greyed out in the bottom panel. Lines and/or symbols show surface sensible heat flux, LCL height and PBL height as indicated, and thin horizontal lines mark daily extremes tailing to the appropriate scale. In the bottom panel, faint or missing hourly markers indicate lack of significance of the anomaly. All significances are at 95% confidence levels.

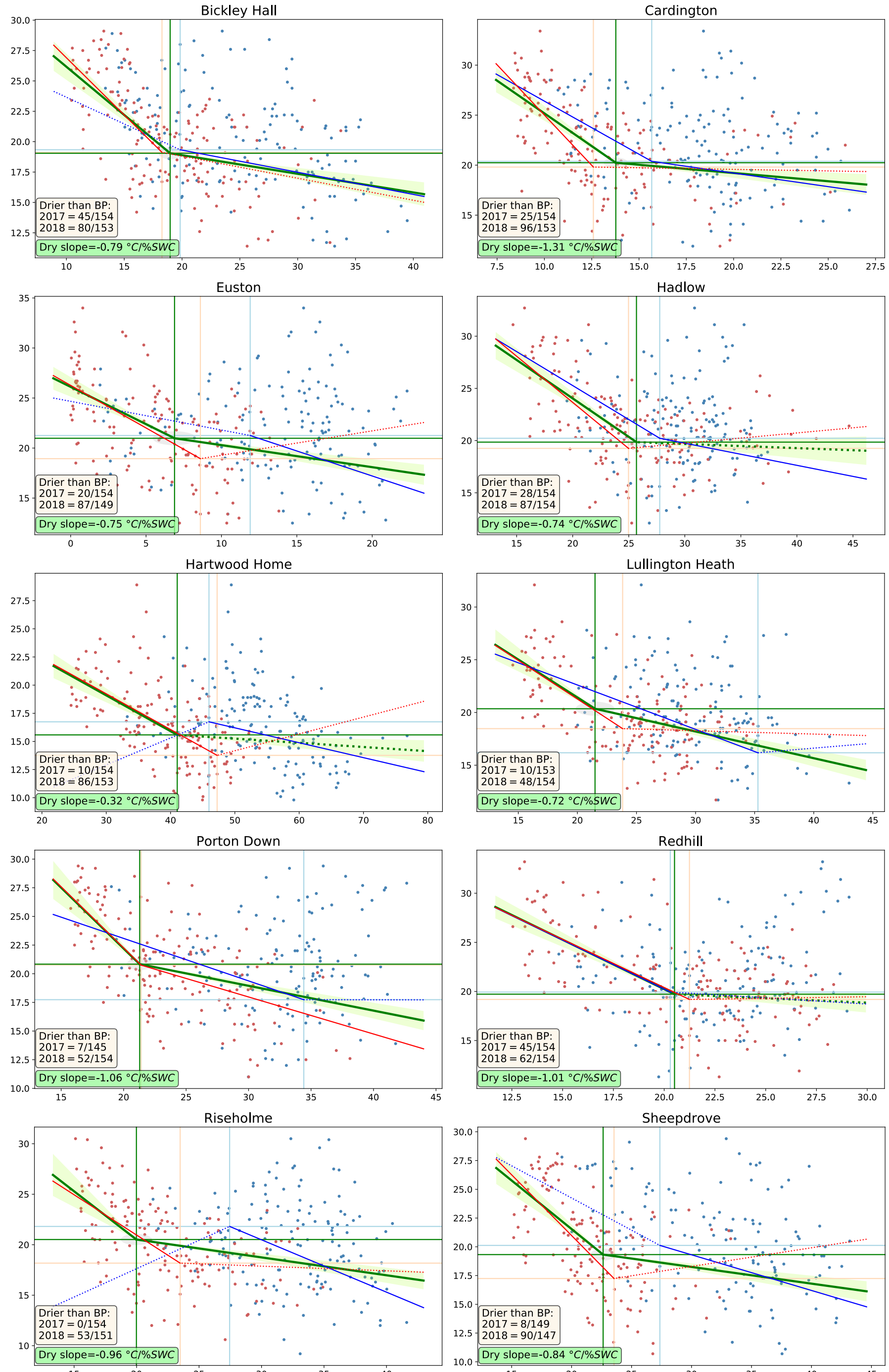

Figure 9: Relationship between daily maximum 2m air temperature (dependent variable; ordinate) and surface volumetric soil water content (abscissa) during 15 May through 15 October for 2017 (blue) and 2018 (red) at indicated COSMOS-UK stations. Breakpoint analysis is performed for each year, and the two years combined (green) where the light shading indicates standard error in the estimate of the slopes. Dotted lines denote slopes that are below the 95% confidence level. A grey ellipse centered on the 2-year breakpoint shows the range of standard error along both axes. Values in the colored boxes show the regression slope (green) and the number of points in each year (tan) on the dry side of the breakpoint.

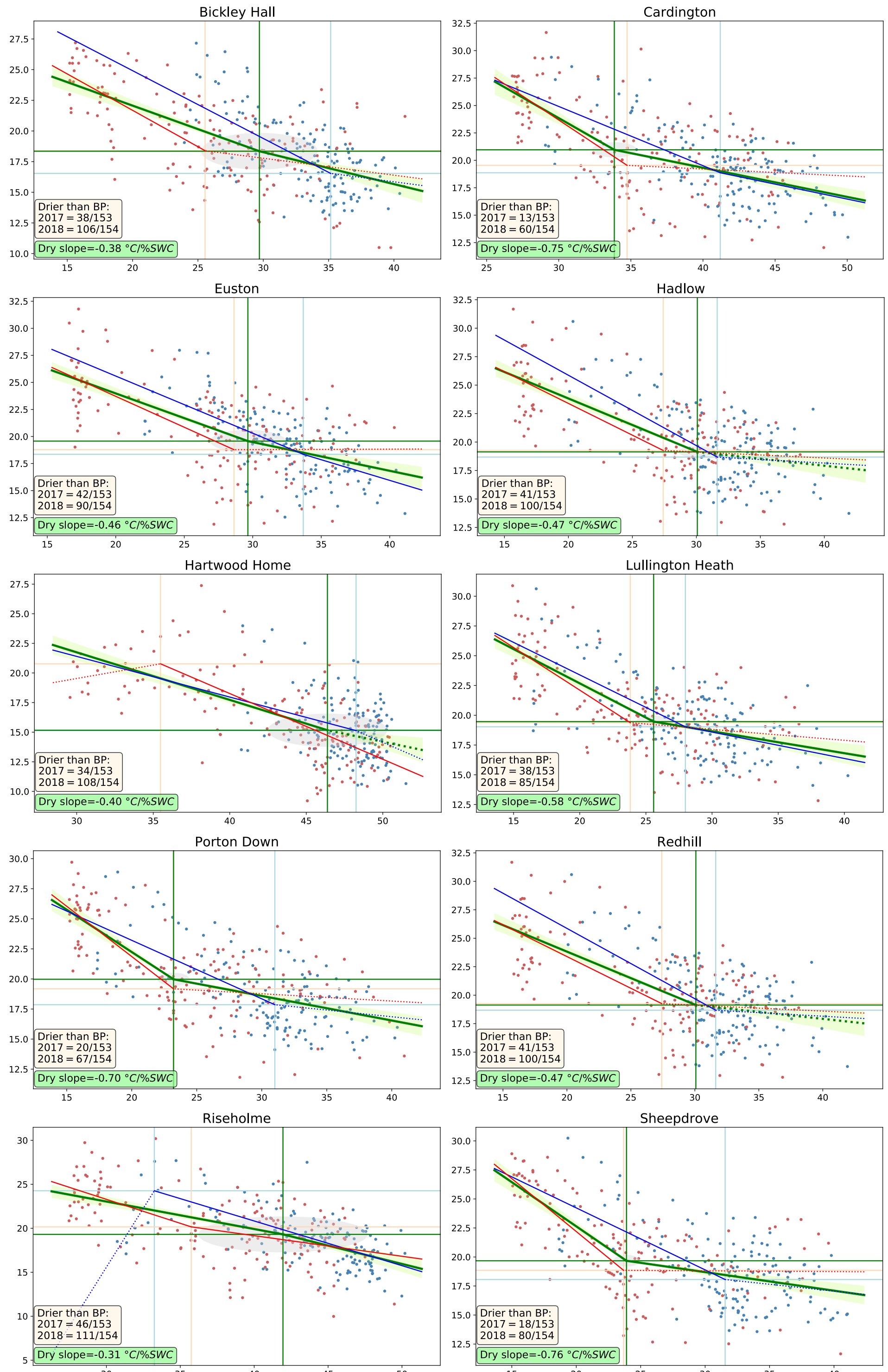

Figure 10: As in Figure 9 for daily ERA5 grid cell data.

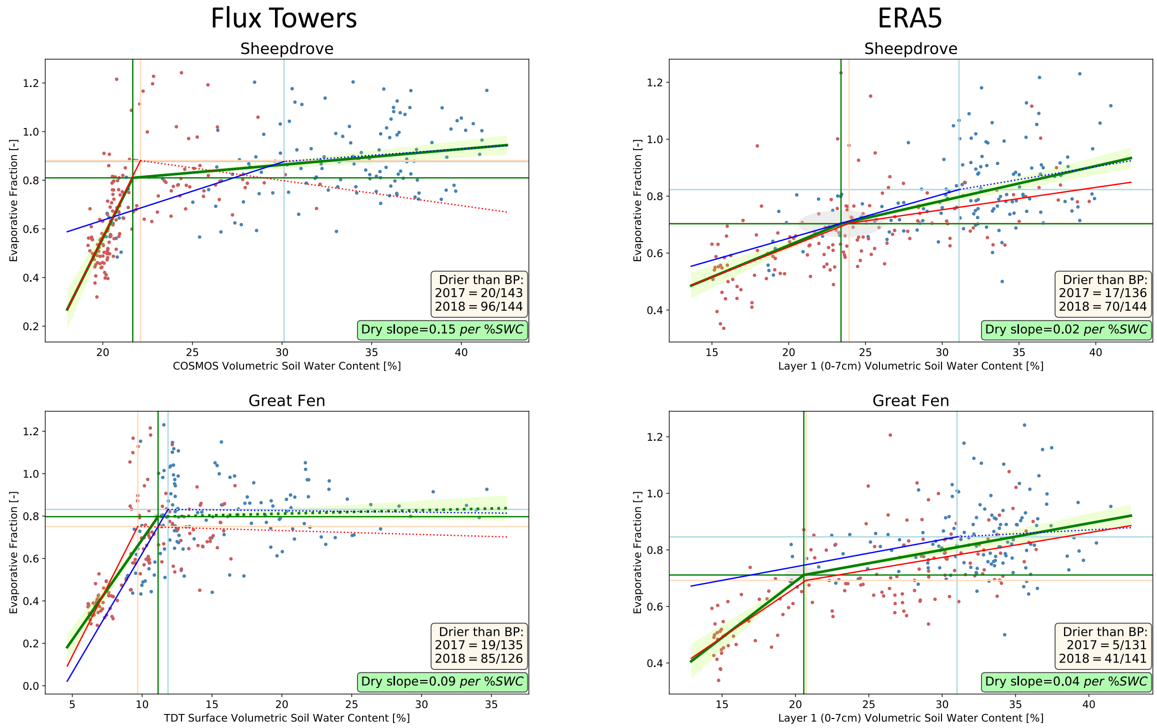

Figure 11: As in Figures 9-10 for breakpoints of evaporative fraction as the dependent variable at flux tower field sites (left column) and ERA5 grid cells encompassing the sites (right column).

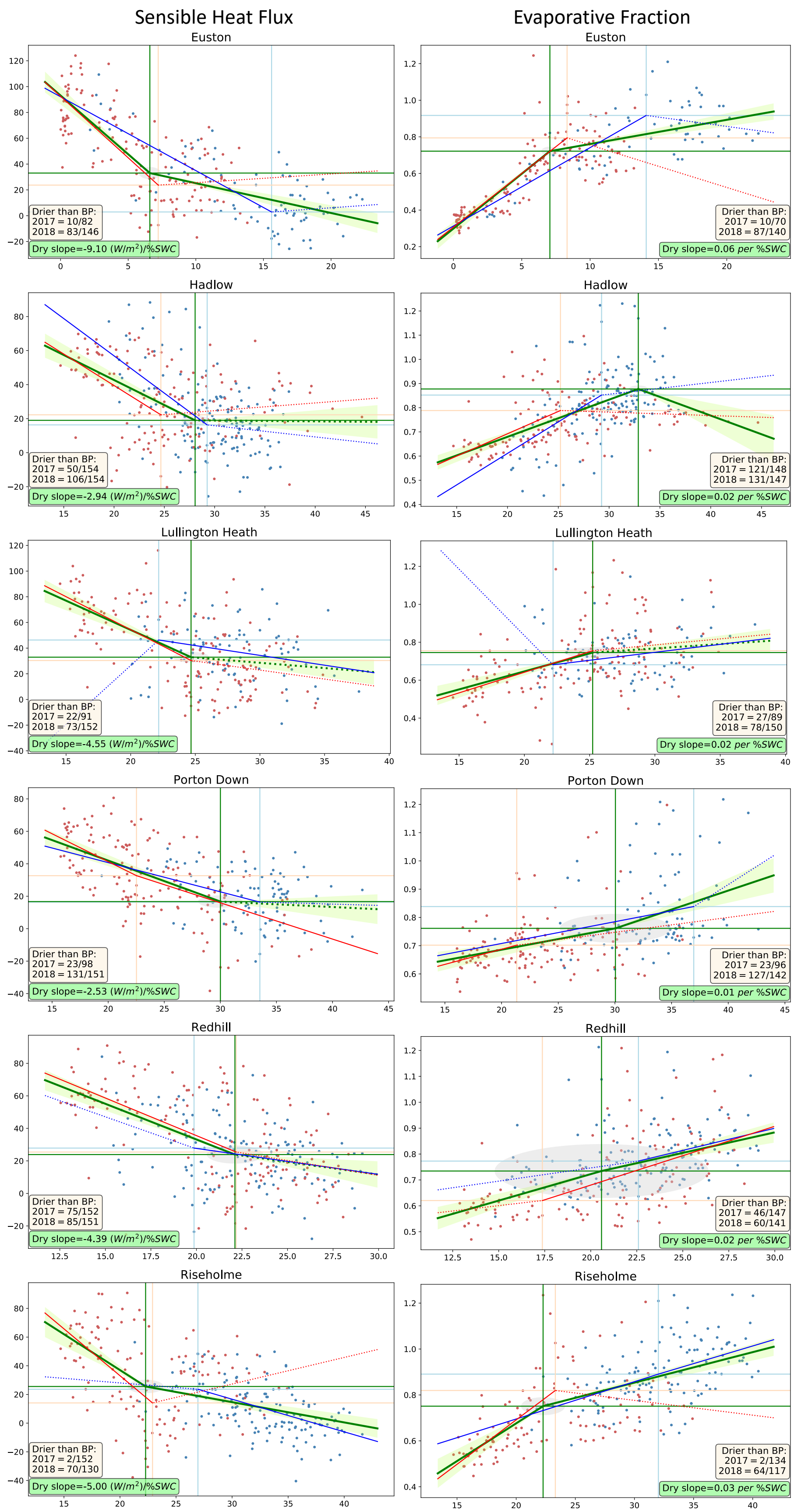

Figure 12: As in Figure 11 for COSMOS-UK sites with estimated surface heat fluxes: sensible heat in the left column (ordinate) and evaporative fraction in the right column (ordinate) versus surface volumetric soil water content (abscissa in both columns).

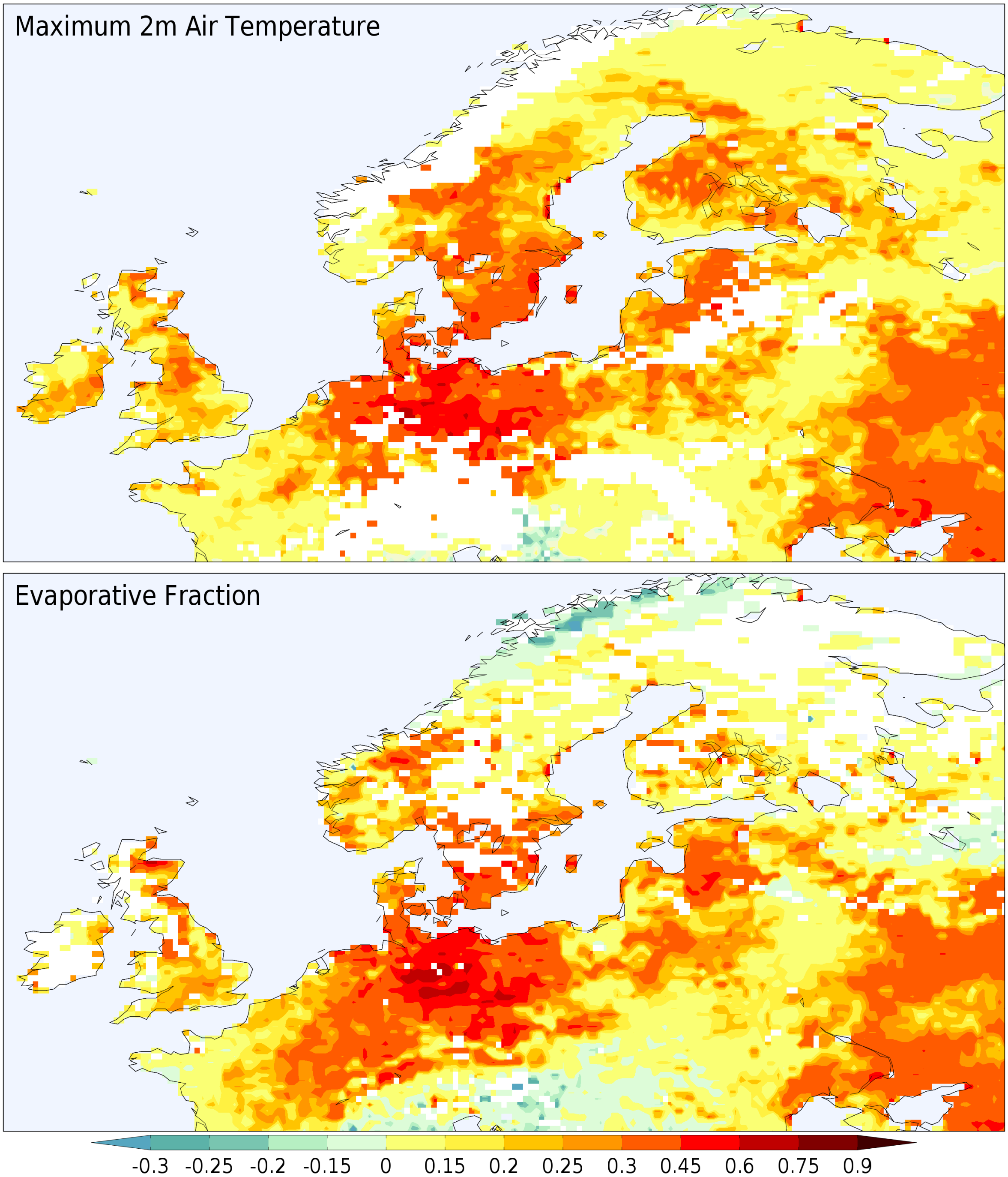

Figure 13: Increase in the fraction of days during May-August on the dry side of the surface volumetric soil water content breakpoint based on ERA5 daily maximum temperature (top) and evaporative fraction (bottom) compared to the 1979-2018 average. Masked areas fail to meet the screening criteria described in Section 3 in all four months.